

To What Extent Can Raindrop Size Be Determined by a Multiple-Frequency Radar?

JONATHAN P. MEAGHER AND ZIAD S. HADDAD

Jet Propulsion Laboratory, California Institute of Technology, Pasadena, California

(Manuscript received 3 March 2005, in final form 15 August 2005)

ABSTRACT

In this paper, an analytical treatment of the atmospheric remote sensing problem of determining the raindrop size distribution (DSD) with a spaceborne multifrequency microwave nadir-looking radar system is presented. It is typically assumed that with two radar measurements at different frequencies one ought to be able to calculate two state variables of the DSD: a bulk quantity, such as the rain rate, and a distribution shape parameter. To determine if this nonlinear problem can indeed be solved, the DSD is modeled as a Γ distribution and quadratic approximations to the corresponding radar–rain relations are used to examine the invertibility of the resulting system of equations in the case of two as well as three radar frequencies. From the investigation, it is found that for regions of DSD state space multiple solutions exist for two or even three different frequency radar measurements. This should not be surprising given the nonlinear coupled nature of the problem.

1. Introduction

An accurate quantitative description of the spatial distribution of precipitation within a mesoscale system requires one to specify not just the rain rate (or precipitating liquid water content) with a high three-dimensional resolution, but also the raindrop size distribution, or at least its mean and variance. In the context of cloud-resolving models, hydrometeor size crucially affects the dynamics of the simulated systems, and in particular the time scale of latent heating release (Ferrer et al. 1995; McCumber et al. 1991). The latter is an essential component of the cumulus parameterizations used in large-scale circulation models. In the context of hydrology, the accurate retrieval of instantaneous surface rain rates from spaceborne sensors is sensitive to hydrometeor size because the relations between the microwave measurements and the underlying precipitation have a significant dependence on drop size (Meneghini et al. 1992; Coppens and Haddad 2000).

A number of precipitation retrieval methods (Goldhirsh and Katz 1974; Goldhirsh 1975; Meneghini et al. 1992) have been proposed that use dual-frequency radar systems to estimate the rain rate R along with a

single drop size distribution parameter. The methods are based on the heuristic idea that if one has simultaneous radar reflectivity measurements at two distinct frequencies one ought to be able to estimate two precipitation state variables. Implicit therein is the assumption that the radar–rain correspondence is one-to-one, that is, that any given pair of reflectivities (Z_1, Z_2) is produced by a single (R, δ) pair, where we have called “ δ ” the DSD parameter that one then hopes to estimate along with R .

A brief examination of the simplest DSD model reveals that the one-to-one assumption is tenuous. Indeed, for an exponential DSD (Marshall and Palmer 1948)

$$N(D)dD = N_0 e^{-\Lambda D} dD \text{ drops of diameter } D \text{ per cubic millimeter,} \quad (1)$$

the equivalent radar reflectivity factors at two distinct frequencies f_1 and f_2 are given by

$$Z_i = \frac{\lambda_{(i)}^4}{\pi^5 |K_w^{(i)}|^2} N_0 \int_0^\infty \sigma_b^{(i)}(D) e^{-\Lambda D} dD, \quad (2)$$

where N_0 is the y intercept and Λ is the slope parameter. Here $\sigma_b^{(i)}(D)$ is the backscattering cross section of

Corresponding author address: Dr. Jonathan P. Meagher, 300-243, JPL, 4800 Oak Grove Drive, Pasadena, CA 91109-8099.
E-mail: meagher@jpl.nasa.gov

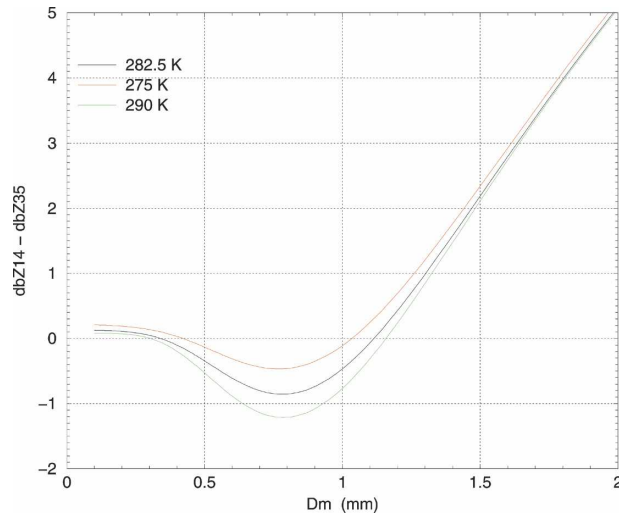


FIG. 1. Ratio $Z_{14\text{GHz}}/Z_{35\text{GHz}}$ vs the mass-weighted mean drop diameter $D_m (=4/\Lambda)$ in the case of the exponential DSD model.

a sphere of liquid water of diameter D and $K_w^{(i)}$ is the dielectric factor of water at frequency f_i ($i = 1, 2$) or wavelength $\lambda_{(i)}$. Mie scattering code is used to calculate $\sigma_b^{(i)}$ values. The ratio Z_1/Z_2 depends on Λ only, though the relation is clearly nonlinear and therefore not necessarily invertible.

Figure 1 illustrates the problem when the two frequencies are those of the proposed Global Precipitation Measurement (GPM) mission's core radar, namely, 14 and 35 GHz. The choice of frequencies of 14 GHz and above is because of the cost and weight constraints placed on space-based radar systems, in particular the antenna. Even if the exact temperature of the rainwater were known, for values of Λ corresponding to a mass-weighted mean drop diameter D_m [which is equal to $4/\Lambda$ (Haddad et al. 1997)] smaller than 1.2 mm, any measurement of the ratio Z_1/Z_2 would correspond to two distinct values of Λ and, hence, two different DSDs. On the other hand, when the mass-weighted mean drop size is greater than 1.2 mm, the simple exponential model suggests that it should indeed be possible to retrieve the rain rate as well as the DSD shape parameter. The goal of this paper is to examine the problem with more realism in the description of the DSD, and for different frequency combinations. Section 2 examines the dual-frequency problem, and section 3 examines the case of a three-frequency radar.

2. Dual-frequency radar

To derive analytic equations for the dependence of the radar reflectivity on the DSD, we start by modeling the latter as a Γ distribution

$$N(D) = N_0 D^\mu e^{-\Lambda D}, \quad (3)$$

and we replace N_0 , μ , and Λ by a set of uncorrelated parameters, namely, the rain rate R , the rain-normalized mass-weighted mean drop diameter $D'' (=D_m/R^{0.15})$, and the rain-normalized mass-weighted DSD width s'' (see Haddad et al. 1997) so that

$$\mu = \frac{1}{s''^2 D''^{0.33} R^{0.074}} - 4, \quad (4)$$

$$\Lambda = \frac{1}{s''^2 D''^{1.33} R^{0.23}}, \quad \text{and} \quad (5)$$

$$N_0 = 55 \frac{\Lambda^{\mu+4}}{\Gamma(\mu+4)[1 - (1 + 0.53/\Lambda)^{-\mu-4}]} R. \quad (6)$$

That (R, D'', s'') are uncorrelated is important because it allows us to fix the values of s'' and D'' and vary R in order to obtain one Z - R relation for every pair of values (D'', s'') at any given frequency.

While power-law approximations to the relation between Z and R have been frequently used (see, e.g., Battan 1973), such relations were generally intended for ground-based radar systems with wavelengths in the Rayleigh scattering regime for raindrop-sized scatterers. For the present application to the higher frequencies typical of spaceborne radars, we have made two extensions to the standard power laws. First, because there is an appreciable curvature in the $\log(Z)$ - $\log(R)$ relations at rain rates below 2 mm h^{-1} , we decided to perform a quadratic approximation to each $\log(Z)$ - $\log(R)$ relation (instead of the linear fits that produce power laws). Second, we had to account for the non-negligible absorption within a radar resolution volume in the calculation of Z . For example, the attenuation coefficient k at 35 GHz for liquid water is roughly $k = 0.2R \text{ dB km}^{-1}$ (with R in millimeters per hour), and it is much higher at higher frequencies such as the Cloud-Sat radar's 94 GHz. This implies that a modest 3 mm h^{-1} of rain would attenuate a 35-GHz wave during its roundtrip propagation through a nominal 250-m radar resolution volume by about 0.3 dB, a nonnegligible amount. The way we accounted for this effect is explained in the appendix. Because the rain-normalized mass-weighted DSD width s'' was found to vary very little (it stays within 10% of its average value of 0.39 for 95% of all DSDs sampled), we decided to fix s'' at its mean value of 0.39, so that the parameters of the relations between Z and R [or, rather, between dBZ and $r = \ln(R)$] depend only on D'' .

We thus have to determine if the system

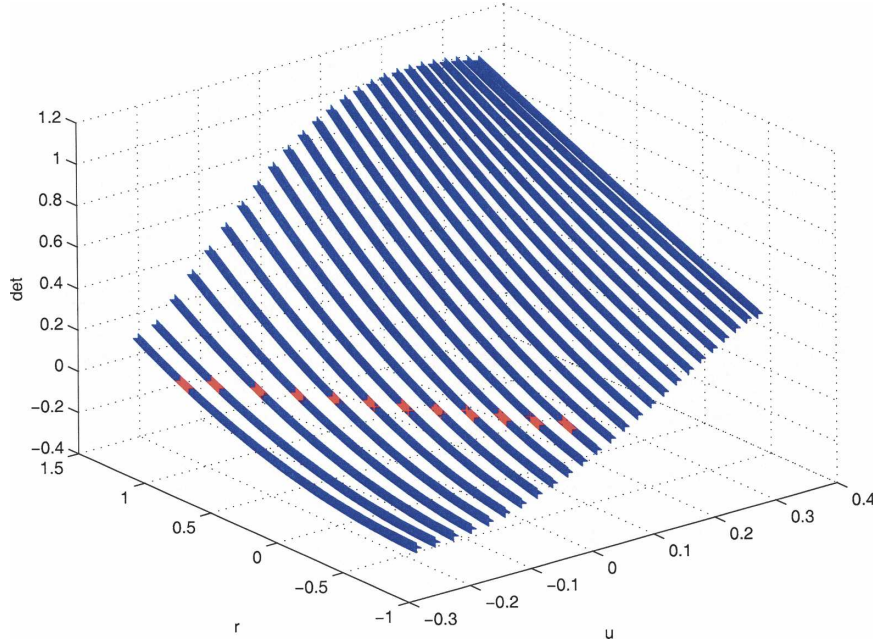


FIG. 2. Jacobian of (Z_{14}, Z_{35}) as a function of the variables $r = \ln(R)$ and $u = \ln(D'')$; $\det = 0$ locations are marked by red points.

$$\begin{aligned}
 Z_1 = \ln(Z_1) &= [a_1(D'') + b_1(D'')r + c_1(D'')r^2] \\
 &+ \ln\left(\frac{1 - e^{-2q\rho_1}}{2q\rho_1}\right) - 2C_1 \quad \text{and} \\
 Z_2 = \ln(Z_2) &= [a_2(D'') + b_2(D'')r + c_2(D'')r^2] \\
 &+ \ln\left(\frac{1 - e^{-2q\rho_2}}{2q\rho_2}\right) - 2C_2
 \end{aligned} \tag{7}$$

admits a unique solution pair (r, D'') . Here, Z_1 and Z_2 are the equivalent radar reflectivity factors measured from a given radar resolution volume, (a_i, b_i, c_i) are the coefficients of the quadratic $\text{dBZ}-r$ relation at the i th frequency, $\rho = \Delta e^{\alpha + \beta r + \gamma r^2}$ with $(\alpha_i, \beta_i, \gamma_i)$ the coefficients of the quadratic $k-r$ relation at the i th frequency and Δ the thickness of the radar volume, q is the constant $0.1 \ln(10)$, and C is the integrated attenuation from the layers between the radar and the current resolution volume (assumed known). The functions a, b, c, α, β , and γ are obtained using quadratic regressions as described in Meagher (2002), with the Z and k values calculated by integrating realizations of the DSD model with Mie code.

Because the system is far from being linear in r and D'' , to determine whether the system is one to one is equivalent to determining if it is invertible. The inverse function theorem states that for a smooth function if the Jacobian is invertible at some point then there exists a smooth inverse in a neighborhood around that

point (Rudin 1976). Hence, one needs to check if the determinant of the Jacobian is nonzero, that is, if

$$\begin{vmatrix} \frac{\partial Z_1}{\partial u} & \frac{\partial Z_1}{\partial r} \\ \frac{\partial Z_2}{\partial u} & \frac{\partial Z_2}{\partial r} \end{vmatrix} \neq 0, \tag{8}$$

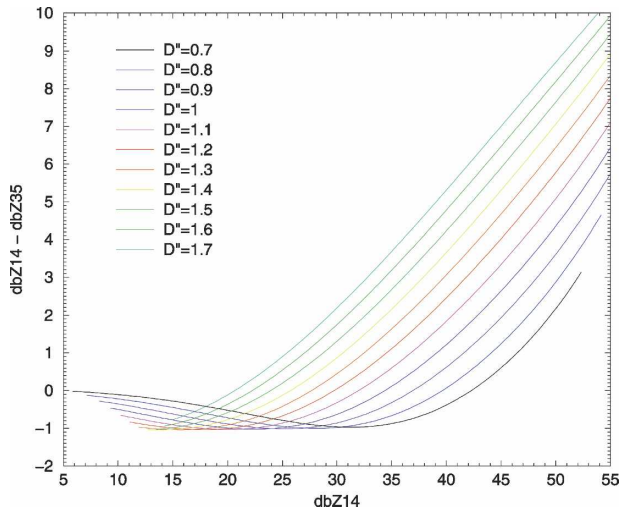


FIG. 3. The (Z_{14}, Z_{35}) values corresponding to different DSDs. Each curve corresponds to a fixed value of $D_m/R^{0.15}$ ($=D''$), with R varying along the curve. The ambiguous region is identified as the area of curve crossing.

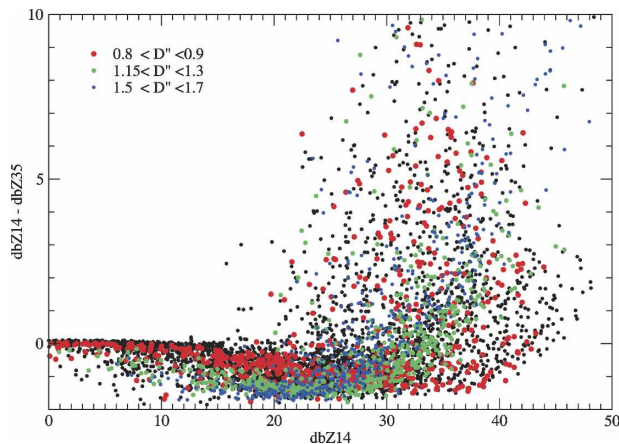


FIG. 4. The (Z_{14}, Z_{35}) calculated from TOGA COARE DSD data using Mie scattering code. One can distinguish the “curve crossing” phenomenon as in Fig. 3 despite the scatter.

where $Z = \ln(Z)$, $r = \ln(R)$, and $u = \ln(D'')$. Figure 2 is a plot of the determinant, that is, the left-hand side of (8). The points in red are the ones where the determinant vanishes and near which the system is not invertible.

Figures 3 and 4 illustrate the ambiguity by showing the dependence of the reflectivity factors on R and D'' . Figure 3 shows how a single (Z_{14}, Z_{35}) measurement can be explained by two distinct (D'', R) pairs in the region where $\text{dbZ}_{14} < 30$ and $\text{dbZ}_{14} < \text{dbZ}_{35}$. All points in this “ambiguous” region have R values smaller than 6 mm h^{-1} .

Figure 4 confirms this “curve crossing” phenomenon with DSD samples collected during the Tropical Ocean and Global Atmosphere Coupled Ocean–Atmosphere Response Experiment (TOGA COARE). Clearly, at lighter rain rates the (14, 35 GHz) system is not one to one, that is, the two frequency channels cannot unambiguously determine the rain rate and one drop size distribution parameter. This is not surprising, because lighter rain rates imply smaller drops, and the reflectivities of smaller drops are not sufficiently different at 14 and 35 GHz. While the difference between the attenuation factors at the two frequencies may be more substantial, the magnitude of the attenuation over a single resolution volume is not sufficiently large to be exploitable in the inversion.

Different choices of frequencies can be considered by calculating their corresponding Jacobian, (8). We shall, however, proceed directly to examining a triple-frequency system, because alternate dual-frequency combinations are considered as part of the triple-frequency analysis.

3. Triple-frequency radar

A possible solution to the ambiguity of the dual-frequency system is to add a third frequency channel and again check the system for multiple solutions. Both 24 and 94 GHz have been proposed as suitable frequencies for atmospheric hydrometeor remote sensing: 94 GHz being the frequency used for the CloudSat Cloud

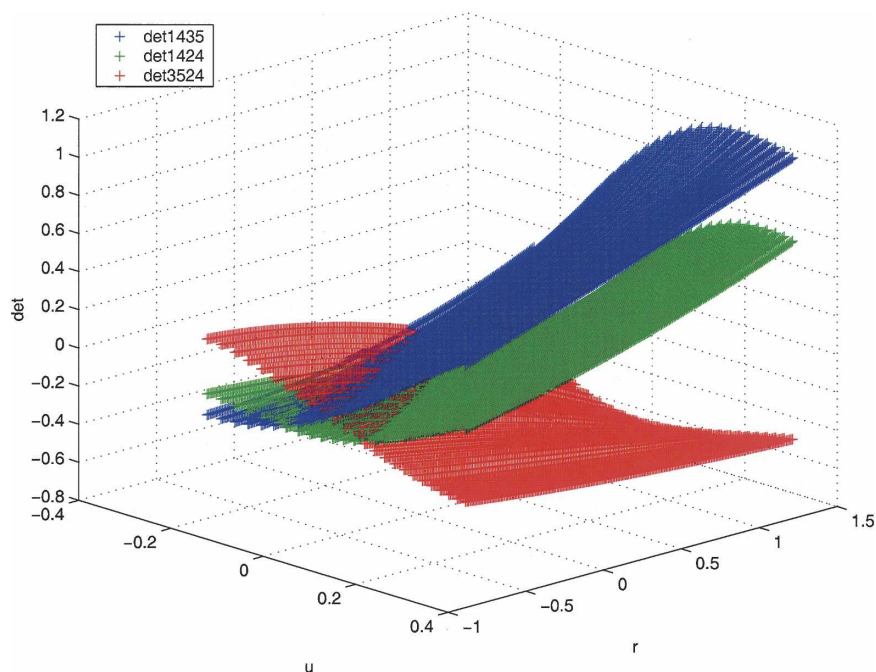


FIG. 5. Determinants for the different combinations of 14-, 24-, and 35-GHz channels.

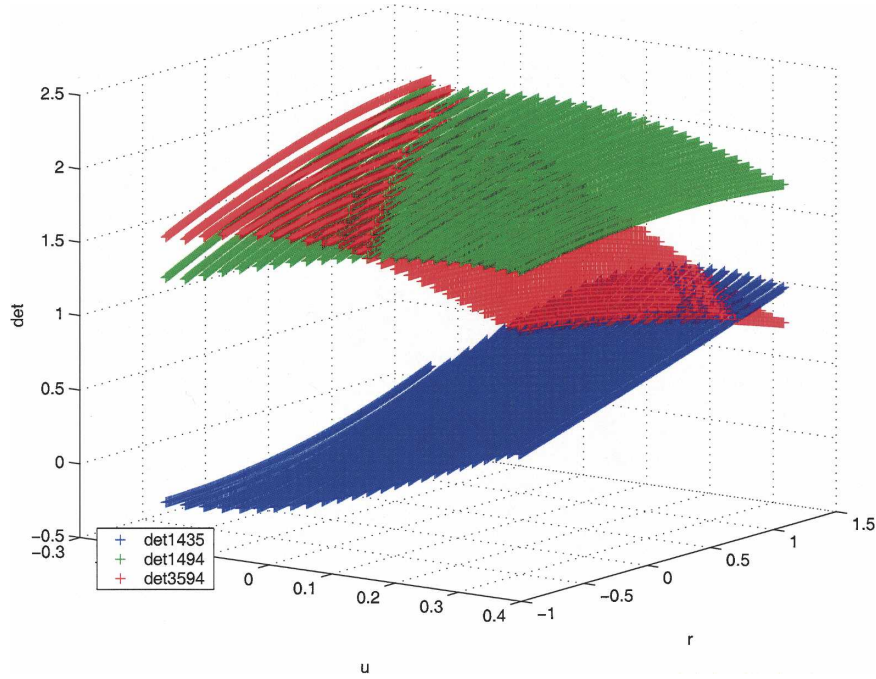


FIG. 6. Determinants for the different combinations of 14-, 35-, and 94-GHz channels.

Profiling Radar (CPR) (Li et al. 2000) and 24 GHz being initially proposed as a second frequency for the Tropical Rainfall Measuring Mission (TRMM) radar system (Simpson 1988).

A radar with three frequencies leads to a system similar to (7), which must be checked for multiple solutions. The Jacobian for a three-frequency system is

$$\begin{pmatrix} \frac{\partial Z_1}{\partial u} & \frac{\partial Z_1}{\partial r} \\ \frac{\partial Z_2}{\partial u} & \frac{\partial Z_2}{\partial r} \\ \frac{\partial Z_3}{\partial u} & \frac{\partial Z_3}{\partial r} \end{pmatrix}, \quad (9)$$

a matrix whose rank depends on the three minors

$$\begin{vmatrix} \frac{\partial Z_1}{\partial u} & \frac{\partial Z_1}{\partial r} \\ \frac{\partial Z_2}{\partial u} & \frac{\partial Z_2}{\partial r} \end{vmatrix}, \quad \begin{vmatrix} \frac{\partial Z_1}{\partial u} & \frac{\partial Z_1}{\partial r} \\ \frac{\partial Z_3}{\partial u} & \frac{\partial Z_3}{\partial r} \end{vmatrix}, \quad \text{and} \quad \begin{vmatrix} \frac{\partial Z_2}{\partial u} & \frac{\partial Z_2}{\partial r} \\ \frac{\partial Z_3}{\partial u} & \frac{\partial Z_3}{\partial r} \end{vmatrix}, \quad (10)$$

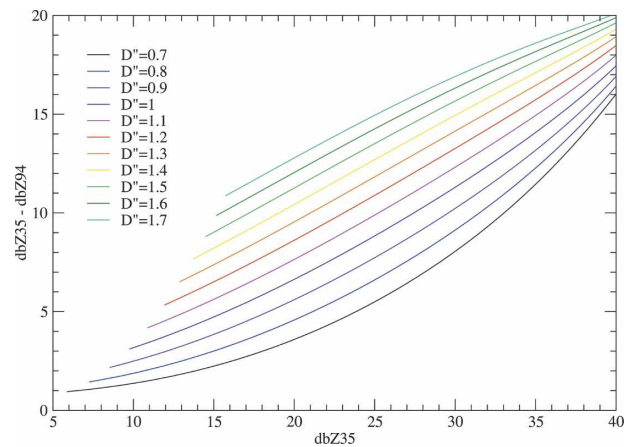
with a minor M_{ij} being the reduced determinant of a determinant expansion that is formed by omitting the i th row and j th column of a matrix. We shall consider two three-frequency combinations, 14 and 35 GHz along with either 24 or 94 GHz.

Figure 5 shows the surfaces for the three determinants (10) for 14, 24, and 35 GHz. Because all three

surfaces cross the ru plane none of the three possible two-frequency combinations would allow for an unambiguous inversion.

While the inclusion of a 24-GHz channel adds little useful information for the unambiguous determination of D'' and R , including a 94-GHz channel does improve the prospects for an unambiguous retrieval. Figure 6 shows that the Jacobian surfaces corresponding to 94 GHz are well removed from the ru plane.

Figure 7 shows how a single (Z_{35}, Z_{94}) measurement should correspond to a single (D'', R) in our DSD

FIG. 7. The (Z_{35}, Z_{94}) values corresponding to different DSDs. Each curve corresponds to a fixed value of $D_m/R^{0.15}$ ($=D''$), with R varying along the curve.

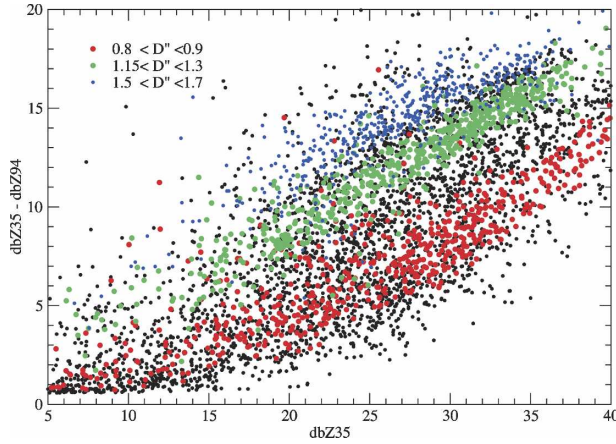


FIG. 8. The (Z_{35}, Z_{94}) calculated from TOGA COARE DSD data using Mie scattering code.

model, and Fig. 8 confirms this observation with DSD samples collected during the TOGA COARE experiment. This would seem to imply that the dual-frequency combinations (14, 94 GHz) and (35, 94 GHz) should allow for the determination of the rain rate as well as the mean drop size.

However, (7) ignores the attenuation resulting from cloud-sized particles, and the latter can definitely not be ignored at 94 GHz. In fact, if we approximate the cloud droplet distribution as a bimodal mixture of typically small (10 μm) and large (70 μm) droplets, Mie scattering shows that the attenuation resulting from these cloud particles is (Meagher 2002)

$$k_c = \mu(1 + g\gamma_c)M_c \text{ dB km}^{-1}, \quad (11)$$

where M_c is the cloud liquid water (g m^{-3}), and $\gamma_c = (\text{mass of large droplets})/(\text{mass of all droplets})$ is the cloud mass fraction that comes from drizzle-sized drops, which we shall consider here to be a parameter (as opposed to an additional variable to be determined from the measurements). The values for the constants (μ, g) at 14, 35, and 94 GHz are $\mu_{14} = 0.14$ and $g_{14} = 0.0038$, $\mu_{35} = 0.83$ and $g_{35} = 0.007$, and $\mu_{94} = 4.47$ and $g_{94} = 0.016$, respectively. Thus, even a monodisperse liquid cloud of 10- μm droplets with a modest 0.15 g m^{-3} water content would attenuate a 94-GHz signal by over 0.3 dB through a nominal 250-m radar resolution volume.

Accounting for the cloud attenuation, our reflectivity equation in (7) becomes

$$Z = [a(D'') + b(D'')r + c(D'')r^2] + \ln\left(\frac{1 - e^{-2q\rho}}{2q\rho}\right) - q\mu(1 + g\gamma_c)M_c\Delta - 2C, \quad (12)$$

and the Jacobian for the three-frequency system

$$\begin{pmatrix} \frac{\partial Z_{14}}{\partial u} & \frac{\partial Z_{14}}{\partial r} & \frac{\partial Z_{14}}{\partial M_c} \\ \frac{\partial Z_{35}}{\partial u} & \frac{\partial Z_{35}}{\partial r} & \frac{\partial Z_{35}}{\partial M_c} \\ \frac{\partial Z_{94}}{\partial u} & \frac{\partial Z_{94}}{\partial r} & \frac{\partial Z_{94}}{\partial M_c} \end{pmatrix} \quad (13)$$

is therefore proportional to

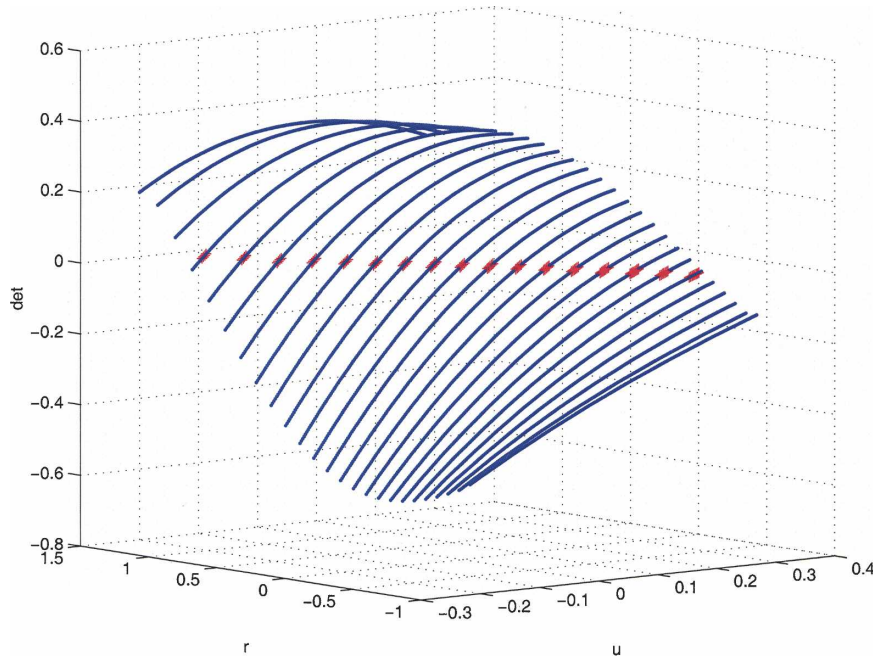


FIG. 9. Jacobian of (Z_{14}, Z_{35}, Z_{94}) including cloud attenuation, assuming a large-droplet cloud mass fraction $\gamma_c = 10\%$; $\det = 0$ locations are marked by red points.

$$\mu_{35}(1 + g_{35}\gamma_c) \begin{vmatrix} \frac{\partial Z_{14}}{\partial u} & \frac{\partial Z_{14}}{\partial r} \\ \frac{\partial Z_{94}}{\partial u} & \frac{\partial Z_{94}}{\partial r} \end{vmatrix} - \mu_{94}(1 + g_{94}\gamma_c) \begin{vmatrix} \frac{\partial Z_{14}}{\partial u} & \frac{\partial Z_{14}}{\partial r} \\ \frac{\partial Z_{35}}{\partial u} & \frac{\partial Z_{35}}{\partial r} \end{vmatrix} - \mu_{14}(1 + g_{14}\gamma_c) \begin{vmatrix} \frac{\partial Z_{35}}{\partial u} & \frac{\partial Z_{35}}{\partial r} \\ \frac{\partial Z_{94}}{\partial u} & \frac{\partial Z_{94}}{\partial r} \end{vmatrix}. \quad (14)$$

Clearly, because (12) is linear in M_c , the Jacobian only depends on variables r and u , that is, on R and D'' . Its dependence on the large-droplet mass fraction γ_c is weak, because the magnitudes of the coefficients g are quite small. Moreover, because μ_{94} is much larger than μ_{14} and μ_{35} , one would expect that the value of the Jacobian would be very close to that of the (Z_{14}, Z_{35}) minor, that is, that its dependence on R and D'' will be very similar to the behavior of the Jacobian of the (14, 35 GHz) dual-frequency system. Figure 9 plots (14) for $\gamma_c = 0.1$. We have verified that the surfaces corresponding to different values of γ_c from 0 to 1 are quite similar; in particular, they all cross the ru plane. This means that the system will not have a unique solution (R, D'', M_c) for a given triple of measured reflectivities.

Thus, if the cloud liquid water content has to be considered an independent variable in addition to the rain-water content and the mean raindrop size, three frequencies are not sufficient to determine the state variables unambiguously. In many cases, such as the wide stratiform areas generated by tropical convection, the cloud liquid water content is typically not substantial enough to contribute significantly to the higher-frequency attenuations (see Fig. 10) and therefore does not warrant being considered an independent variable. In those cases, a dual- or triple-frequency system, including a 94-GHz channel, should be capable of sorting out the rain variables. In other cases, such as incipient tropical convective cells in which cloud liquid cannot be ignored, the three reflectivities are not sufficient to resolve the ambiguities.

4. Conclusions

This study concentrated on the determination of rain characteristics within an individual radar resolution volume. The conclusions presume that the radar channels have sufficient dynamic range to span the possibly large absorption by liquid water at higher frequencies, and that the accumulated attenuation can be accurately tracked through consecutive resolution volumes. Because the reflectivities of smaller raindrops are not sufficiently different at lower frequencies such as 14 and 35 GHz, one can hope for an unambiguous determination of rain rate and mean drop size from a (14, 35 GHz)

dual-frequency radar only if the rain rate is known a priori to be greater than 6 mm h^{-1} . An additional 24-GHz measurement would not be sufficiently independent to help in the retrieval. A (14, 94 GHz) or (35, 94 GHz) system would permit an unambiguous retrieval if the 94-GHz cloud absorption were negligible, that is, if the cloud liquid water content were known a priori to be smaller than 0.15 g m^{-3} . If the cloud liquid has to be considered as an independent variable, the reflectivities at 14, 35, and 94 GHz are not sufficiently independent for the unambiguous determination of rain rate, mean drop size, and cloud liquid water content.

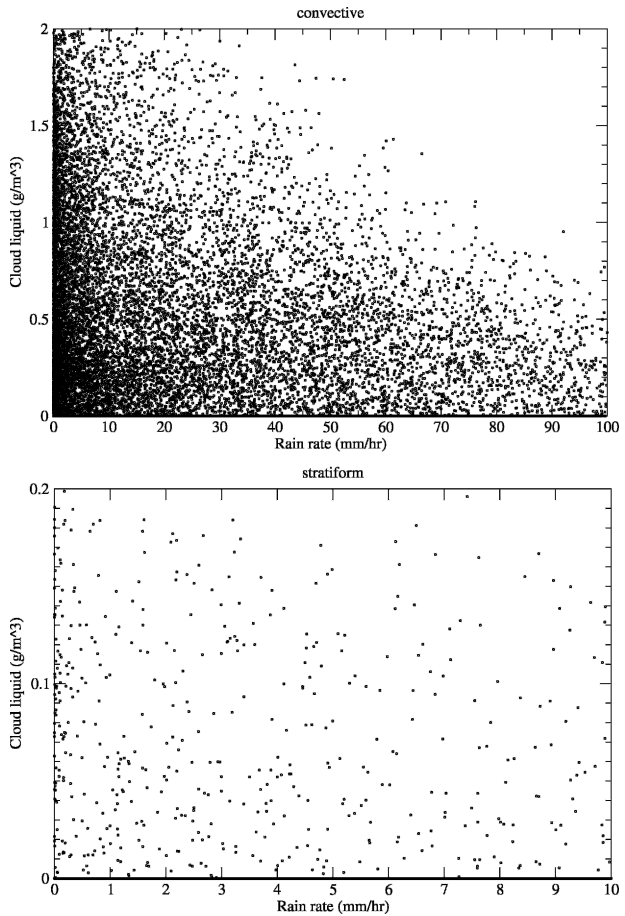


FIG. 10. Cloud liquid vs precipitating liquid (in 700-m-thick layers between the surface and the melting band) according to cloud-resolving simulations of a mesoscale convective system observed during TOGA COARE (Trier et al. 1996): (a) stratiform and (b) convective clouds.

Acknowledgments. This work was performed at the Jet Propulsion Laboratory, California Institute of Technology, under contract with the National Aeronautics and Space Administration.

APPENDIX

Attenuated Reflectivity

Consider a radar resolution volume of thickness Δ starting at height $x = \text{bottom}$ and extending up to $x = \text{top}$, and assume that the reflectivity factor Z and the attenuation coefficient k are constant within the volume. The measured reflectivity Z_m would then be

$$\begin{aligned} Z_m &= \left(e^{-2q \int_0^{\text{top}} k} \right) \frac{1}{\Delta} \int_{\text{top}}^{\text{bottom}} \left(Z e^{-2q \int_{\text{top}}^r k} \right) dr \\ &= Z \left(\frac{1 - e^{-2qk\Delta}}{2qk\Delta} \right) e^{-2q \int_0^{\text{top}} k}, \end{aligned} \quad (\text{A1})$$

with $q = 0.1 \ln(10)$.

REFERENCES

- Battan, L. J., 1973: *Radar Observations of the Atmosphere*. The University of Chicago Press, 324 pp.
- Coppens, D., and Z. Haddad, 2000: Effects of raindrop size distribution variations on microwave brightness temperature calculation. *J. Geophys. Res.*, **105**, 24 483–24 489.
- Ferrier, B., W. Tao, and J. Simpson, 1995: A double-moment multiple-phase four-class bulk ice scheme. Part II: Simulations of convective storms in different large-scale environments and comparisons with other bulk parametrizations. *J. Atmos. Sci.*, **52**, 1001–1033.
- Goldhirsh, J., 1975: Improved error analysis in estimation of rain-drop spectra, rain rate, and liquid water content using multiple wavelength radars. *IEEE. Trans. Antennas Propag.*, 718–720.
- , and I. Katz, 1974: Estimation of raindrop size distribution using multiple wavelength radar systems. *Radio Sci.*, **9**, 439–446.
- Haddad, Z. S., D. A. Short, S. L. Durden, E. Im, S. Hensley, M. B. Grable, and R. A. Black, 1997: A new parametrization of the rain drop size distribution. *IEEE Trans. Geosci. Remote Sens.*, **35**, 532–539.
- Li, F. K., E. Im, S. L. Durden, and R. Girard, 2000: Cloud Profiling Radar (CPR) for the CloudSat mission. *Proc. Geoscience and Remote Sensing Symp.*, Vol. 6, Honolulu, HI, IEEE/IGARSS, 2546–2548.
- Marshall, J., and W. Palmer, 1948: The distribution of rain drops with size. *J. Meteor.*, **5**, 165–166.
- McCumber, M., W. Tao, J. Simpson, R. Penc, and S. Soong, 1991: Comparison of ice-phase microphysical parametrization schemes using numerical simulation of tropical convection. *J. Appl. Meteor.*, **30**, 985–1004.
- Meagher, J. P., 2002: Spaceborne monitoring of cloud and rain hydrometeor size distributions. Ph.D. thesis, University of California, Los Angeles, 200 pp.
- Meneghini, R., T. Kozu, H. Kumagai, and W. C. Boncyk, 1992: A study of rain estimation methods from space using dual-wavelength radar measurements at near-nadir incidence over ocean. *J. Atmos. Oceanic Technol.*, **9**, 364–382.
- Rudin, W., 1976: *Principles of Mathematical Analysis*. 3d ed. McGraw-Hill, 325 pp.
- Simpson, J., 1988: TRMM—A satellite mission to measure tropical rainfall. NASA GSFC Tech. Rep. of the Science Steering Group, 94 pp.
- Trier, S. B., W. C. Skamarock, M. A. LeMone, D. B. Parsons, and D. P. Jorgensen, 1996: Structure and evolution of the 22 February 1993 TOGA COARE squall line: Numerical simulations. *J. Atmos. Sci.*, **53**, 2861–2886.